

Diode Characteristics of Doping-Modulated Multilayers of Amorphous Silicon

I. Chen, H. Steemers, J. Mort, and M. Machonkin

Xerox Webster Research Center

800 Phillips Road, Webster, NY 14580, USA

Charge carrier transport in amorphous semiconductor doping-modulated multilayers, consisting of alternating thin n- and p-type sublayers, in the direction perpendicular to the layer planes has been investigated. Theoretical analyses show that as the sublayer thickness decreases, the multilayers behave like a p-i-n junction diode. Experimental results, obtained with phosphorus or boron doped amorphous hydrogenated silicon multilayers, are presented to confirm the prediction.

1. INTRODUCTION

The fabrication and characterization of multilayers (superlattices) made from amorphous solids have emerged as one of the most active subjects in the field of amorphous semiconductors.¹ In composition-modulated multilayers, e.g. those consisting of alternating layers of undoped amorphous hydrogenated silicon (a-Si:H) and insulators such as silicon oxides, nitrides or carbides, investigations have been mainly aimed at observing a quantum-well effect.² On the other hand, in doping-modulated multilayers, which consist of alternating layers of p- and n-type doped a-Si:H, potential applications as electronic devices seem more promising.

Most electrical and photo-electrical measurements on a-Si:H doping-modulated multilayers reported in the literature³ deal with carrier transport parallel to the layer planes. In this paper, a theoretical and an experimental investigation of carrier transport perpendicular to the layer planes in doping-modulated multilayers of a-Si:H are reported.

It may be conjectured that in doping-modulated multilayers no appreciable current flows in the direction perpendicular to the layer planes, because of the reverse biased junctions at every other interface (independent of the direction of external bias). However, the space-charge doping effect, which arises from charge transfer through

the interfaces, can lower the interfacial potential barriers significantly in these thin film multilayers. In a previous theoretical study of the space-charge doping in a-Si:H multilayers,⁴ the potential distributions (with no bias across the layers) have been calculated as a function of the thickness, the doping levels, and the localized state density of the sublayers. The results have successfully elucidated the experimental observations on the nature of in-layer carrier transport (persistent photoconductivity).

In this paper, the theoretical analysis of the current-voltage relations for a-Si:H doping-modulated multilayers is described in Section 2. The experimental studies are reported in Section 3, and in more detail in a recent publication.⁵

2. THEORY

The current density (perpendicular to the layers) in a-Si:H multilayers of various sublayer thicknesses are calculated from the potential and the quasi-Fermi energy distributions. For the purpose of illustrating the diode characteristics of such devices with minimum mathematical complexity, an idealized symmetric multilayer, shown schematically in Fig.1, is considered. The total thickness of the multilayer is $2L$, consisting of $2N$ sublayers of alternating p- and n-type materials of thickness S , (i.e. $N \times S = L$). The sublayers are doped to the extent that the bulk

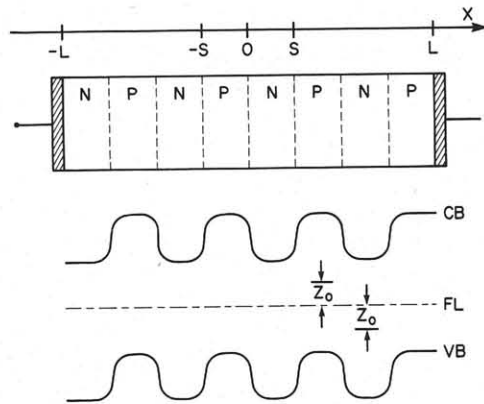


Fig.1 Schematics of the structure of a multilayer with $2N=8$, and the energy band diagram showing the relative positions of conduction band (CB), the valence band (VB), and the Fermi level (FL), at equilibrium.

Fermi levels would be at Z_0 below and above the midgap for the p- and n-type sublayers, respectively. Furthermore, the hole and the electron mobilities are assumed to be equal, and are the same in the p- and n-type sublayers. An extension to general values of hole to electron mobility ratio has little effect on the conclusion.

The steady state current characteristics are governed by the following set of equations,

$$J_h(x) = \mu kT [p(x) dV/dx - dp/dx] \quad (1)$$

$$J_e(x) = \mu kT [n(x) dV/dx + dn/dx] \quad (2)$$

$$dJ_h/dx = -dJ_e/dx = q[G(x) - R(x)] \quad (3)$$

$$d^2V/dx^2 = qQ(x)/\epsilon kT \quad (4)$$

The first two equations are the expressions for the hole and the electron current densities, respectively, where V is the electronic potential energy (in units of kT), μ is the carrier mobility, and p and n are the hole and the electron densities, respectively. The third equation is the continuity equation, where G and R are the rates of carrier generation and recombination, respectively. The last equation is Poisson's equation with Q denoting the space charge density, ϵ the permittivity, and q the elemental charge.

The carrier densities can be expressed in terms of the hole and the electron quasi-Fermi energies, Z_h and Z_e (in units of kT), as,

$$p = n_i \exp[V(x) - Z_h(x)] \quad (5)$$

$$n = n_i \exp[Z_e(x) - V(x)] \quad (6)$$

The quasi-Fermi energies at the terminals, $x = \pm L$, are determined by the applied bias voltage V_b as,

$$Z_h(\pm L) = Z_e(\pm L) = \mp V_b/2 \quad (7)$$

The total current density J is given by the sum of the hole- and the electron- current densities,

$$J = J_h(x) + J_e(x) = J_h(0) + J_e(0) \quad (8)$$

The generation rate G in the continuity equation, Eq.(3), is assumed to be a constant, and and the recombination rate R is given by the Shockley-Read-Hall model,

$$R = (\mu kT/q) [np - n_i^2] / [L_h^2(n+n_i) + L_e^2(p+n_i)] \quad (9)$$

where L_h and L_e are the hole and the electron diffusion lengths, respectively.

In Poisson's equation, Eq.(4), the space charge density $Q(x)$ is given by,

$$Q(x) = q(p - p_0 - n + n_0) + Q_L \quad (10)$$

where the equilibrium densities of holes (p_0) and electrons (n_0) can be expressed in terms of the bulk Fermi energy Z_0 as,

$$p_0 = n_i \exp(-Z_0), \quad n_0 = n_i \exp(Z_0) \quad (11)$$

The contribution from the charge in the localized states, Q_L , takes a simple analytic form if the distributions of the acceptor-like and the donor-like localized states are assumed to be exponential,

$$N_A(E) = N_a \exp(E/E_a) \quad (12)$$

$$N_D(E) = N_d \exp(-E/E_d) \quad (13)$$

where the energy E is measured from the midgap, and E_a and E_d are constant parameters specifying the exponential distributions.

The mathematical procedure for numerical calculations of the current density J by solving the set of differential equations for $V(x)$, $Z_h(x)$, and $Z_e(x)$ is detailed in a separate forthcoming publication.⁶

Fig.2 shows the potential distributions $V(x)$ at equilibrium ($G-R=0$ and $V_b=0$), for three multilayers consisting of 4, 10, and 20 alternatively p- and n-type sublayers, with the total thickness of $2L=1 \mu m$. In the equilibrium state, the electron and the hole quasi-Fermi energies are equal and constant, ($Z_e=Z_h=Z$), and are taken as the origin of the energy axis.

The n-type sublayers are assumed to have the bulk Fermi level at 0.4eV above the midgap. The density of acceptor-like states and the donor-like states are $N_A=10^{15}$ and $N_D=10^{16} \text{ cm}^{-3} \text{ eV}^{-1}$, respectively, at the midgap, and increase exponentially to $3 \times 10^{18} \text{ cm}^{-3} \text{ eV}^{-1}$ at the conduction and the

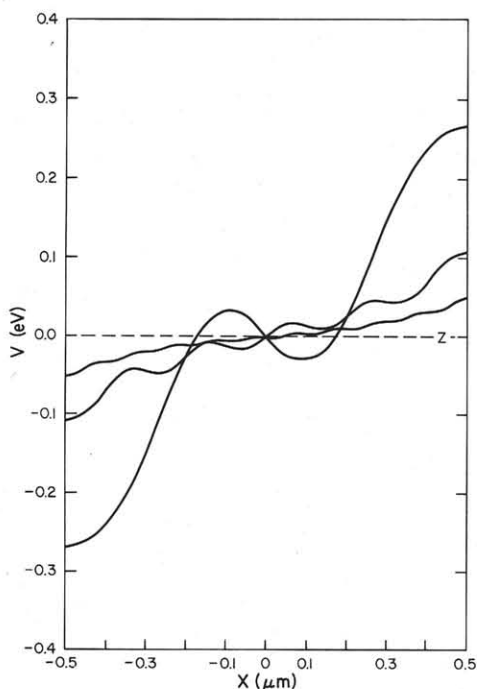


Fig.2 The electronic potential energy distributions at zero bias of three multilayers consisting of (a)4, (b)10, and (c)20 alternatively p- and n-type sublayers.

valence band edges, ($E = \pm 0.75\text{eV}$). This condition determines the parameters E_a and E_d in Eqs.(12,13). In the p-type sublayers, the bulk Fermi level lies 0.4eV below the midgap, and the midgap values of the acceptor-like and the donor-like states are interchanged from those of n-type sublayers. The intrinsic carrier concentration is $n_i = 2 \times 10^7 \text{ cm}^{-3}$.

It can be seen that the inter-layer potential barrier decreases with the sublayer thickness. Physically this means that due to the counter-doping nature of space charge doping, the n-type sublayers become less n-type and the p-type sublayers become less p-type. In the 20-sublayer device, this effect is so large that almost all of the inner sublayers become near intrinsic, or even inverted. Thus, all the right side half of the device is effectively p-type and the left side half is effectively n-type, and the multilayer becomes essentially a single pin junction.

When a bias voltage is applied to the multilayer, the sublayer interfaces are alternately reverse and forward biased, independent of the sign of the bias voltage. In Shockley (npnp) diodes with thick sublayers, no significant current can flow across the multilayer until the switching voltage is reached. This is not the case

in the thin-film multilayers under consideration, because of the barrier lowering due to space charge doping.

To calculate the current density J , one must specify the hole and the electron diffusion lengths, L_h and L_e , respectively. In this model system with symmetric doping, it is assumed that L_h in the p-type layer is equal to L_e in the n-type layer and are denoted as the majority carrier diffusion length, L_{maj} . Similarly, L_h in the n-type layer is assumed to have the same value as L_e in the p-type layer, and are denoted as the minority carrier diffusion length, L_{min} .

The J-V relations calculated with $L_{maj} = 1\mu\text{m}$ and $L_{min} = 0.01\mu\text{m}$ for several multilayers are shown in Fig.3. With forward biases the current increases exponentially as in a pn junction. The quality factor is about 1.9, indicating that recombination current dominates. The two devices A and B have the normal structure of 2N layers of equal thickness S given in the figure caption, and the electronic parameters specified previously. For these two devices, there is some asymmetry in the J-V relation with respect to the direction of the external bias, but not as much a rectifying character as seen in conventional pn diodes. This can be attributed to the decrease in the built-in

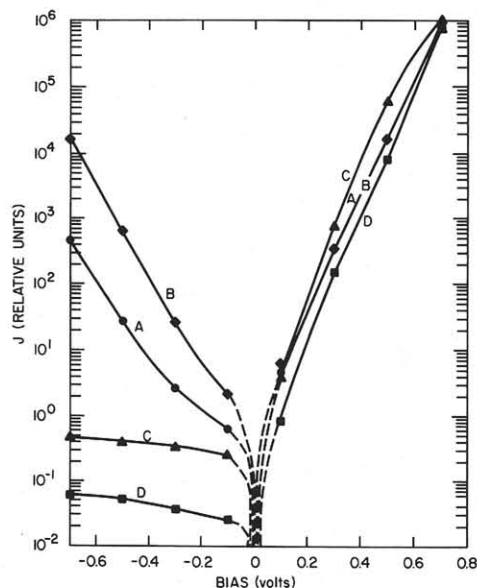


Fig.3 The current-voltage relations calculated for four multilayers (A) $S = 0.1 \mu\text{m}$ and $2N=10$; (B) $S = 0.05 \mu\text{m}$ and $2N=20$; (C) same as (A) except the two outermost sublayers are doubled in thickness. The bulk Fermi energy is $Z = 0.4 \text{ eV}$ for all the above. (D) $S = 0.02 \mu\text{m}$, $2N=10$, and $Z = 0.6 \text{ eV}$.

potential. The built-in potentials for these two devices are 0.2 and 0.1 eV, respectively, compared to the nominal value of 0.8 eV (with the bulk Fermi levels at +0.4 eV).

The built-in potential of a multilayer can be increased, without much affecting the barrier height at the internal junctions, by increasing only the thickness of the outermost sublayers. In device C on Fig.3, the outermost sublayers of device A are doubled in thickness. This increases the built-in potential to 0.52 eV, and an improved rectifying character as shown in Fig.3. Alternatively, with a more highly doped sublayers, e.g. with bulk Fermi levels at +0.6 eV as in device D, one has a built-in potential of 1.1 eV at a sublayer thickness of 0.02 μm , and a significant rectifying character as shown in curve D of Fig.3.

An important feature of the thin-film multilayers distinct from the conventional pn junction (of the same thickness) is the following. Because the counter doping is achieved by space charge rather than by chemical impurities, even in the p-type half there exist regions with low electron-trap density, and similarly there exist regions of low hole-trap density in the n-type half. The impact of this feature on the collection of photo-generated carriers has been analysed theoretically.⁶

3. EXPERIMENTS

The multilayer samples of a-Si:H were prepared in an rf plasma deposition system. The total pressure in the system was maintained at 200 mTorr, and the samples were deposited on Al substrates at 230°C with a power density of 0.06 Wcm⁻³. The doping levels of 9 ppm phosphorus and 100 ppm boron in the n and p-type sublayers, respectively, were chosen so that there is a symmetrical shift of the Fermi level of ~0.4 eV from the mid-gap. The lack of cross-contamination of dopants was assured by SIMS analyses.

The measured current-voltage characteristics of three such samples are shown in Fig.4. All samples have a 0.25 μm bottom- and a top-contact of n- and p-type, respectively. Between the two contacts, there are 2, 6 and 10 alternately doped sublayers of thickness 0.25, 0.1, and 0.05 μm , respectively. At a given bias voltage, the current increases as

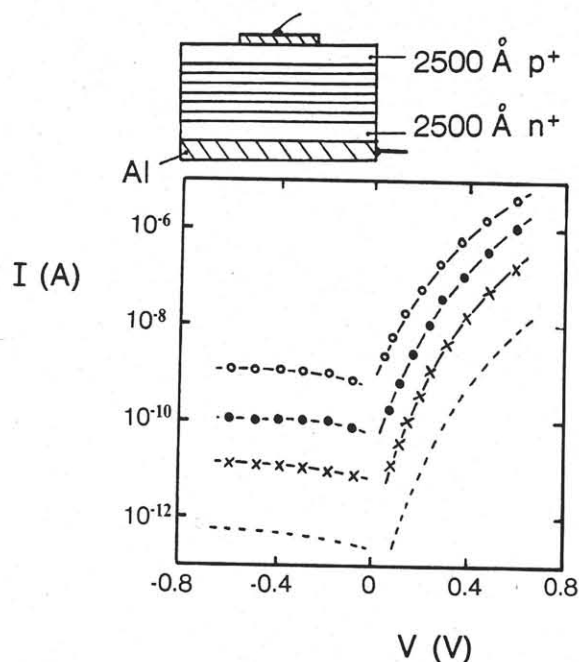


Fig.4 Measured I-V curves for multilayers with sublayer thickness (o) 0.05 μm , (●) 0.1 μm , and (x) 0.25 μm . The broken line represents the data for a deliberately cross-contaminated sample. The sample configuration for I-V measurements is shown at the top.

the sublayer thickness decreases, in agreement with the theoretical predictions of the preceding section. To demonstrate that this is not due to an increase in cross-contamination of the dopants as the sublayer thickness is reduced, a deliberately cross-contaminated sample was made with 9 ppm of P and 100 ppm of B in each sublayer. The result for this sample is shown by the broken lines.

REFERENCES

1. Proceedings of 11-th International Conference on Amorphous and Liquid Semiconductors, Rome, Italy, in J.Non-Cryst. Sol. 77 & 78, (1985)
2. B. Abeles and T.Tiedje, Phys. Rev. Lett. 51, 2003 (1983); T.Tiedje, C.R.Wronski, P.Persans, and B.Abeles, in Ref.1, p.1031
3. J.Kakalios and H.Fritzsche, Phys. Rev. Lett. 53, 1602 (1984); also in Ref.1, p.1101
4. I.Chen, Phys. Rev. B32, 879 and 890 (1985); also in Ref.1, p.1093
5. H.Steemers, I.Chen, J.Mort, F.Jansen, M.Morgan, M.Machonkin and D.Kuhman, Proceedings of 1986 MRS symposium, Palo Alto, Calif.
6. I.Chen, submitted to J. Appl. Physics